Supplemental Information

Electric Double Layer Structure Modulates Poly-dT_{25} Conformation and Adsorption Kinetics at Cationic Lipid Bilayer Interface

PengHua Li,[a, b] Yang Shen,[b] LiQun Wang,[c] WangTing Lu,[a] WenHui Li,[a] Kun Chen,[a] YouHua Zhou,[b] Lei Shen,*[, d] Feng Wei, *[, a] and WanQuan Zheng[a, e]

1. SFG-VS spectra of lipid bilayer in various salt solution.

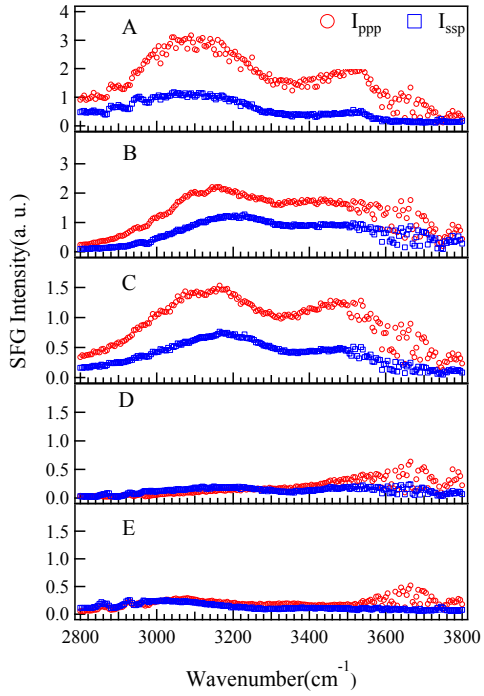

Figure S1 SFG spectra of DMTAP bilayer collected in the wavenumber range of 2800-3800 cm^{-1} at various C_{tris}. A C_{Tris} = 0.1 mM; B . C_{Tris} = 5 mM; C . C_{Tris} = 10 mM; D. C_{Tris} = 25 mM; E. C_{Tris} = 75 mM.

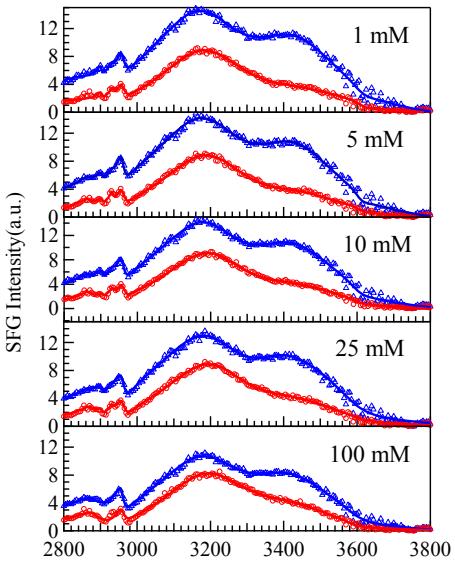

Figure S2 SFG spectra of $(C_{16}H_{33})_2PO_4Cl$ bilayer collected in the wavenumber range of 2800-3800 cm^{-1} at various C_{tris}.

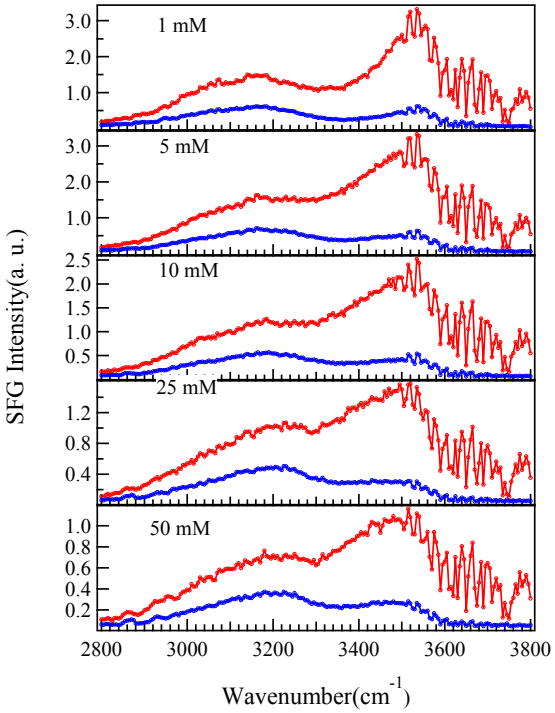

Figure S3 SFG spectra of DMTAP bilayer collected in the wavenumber range of 2800-3800 cm^{-1} at various C_{MgCl2}.

2. SFG intensity ratio of poly-dT_{25} adsorption process

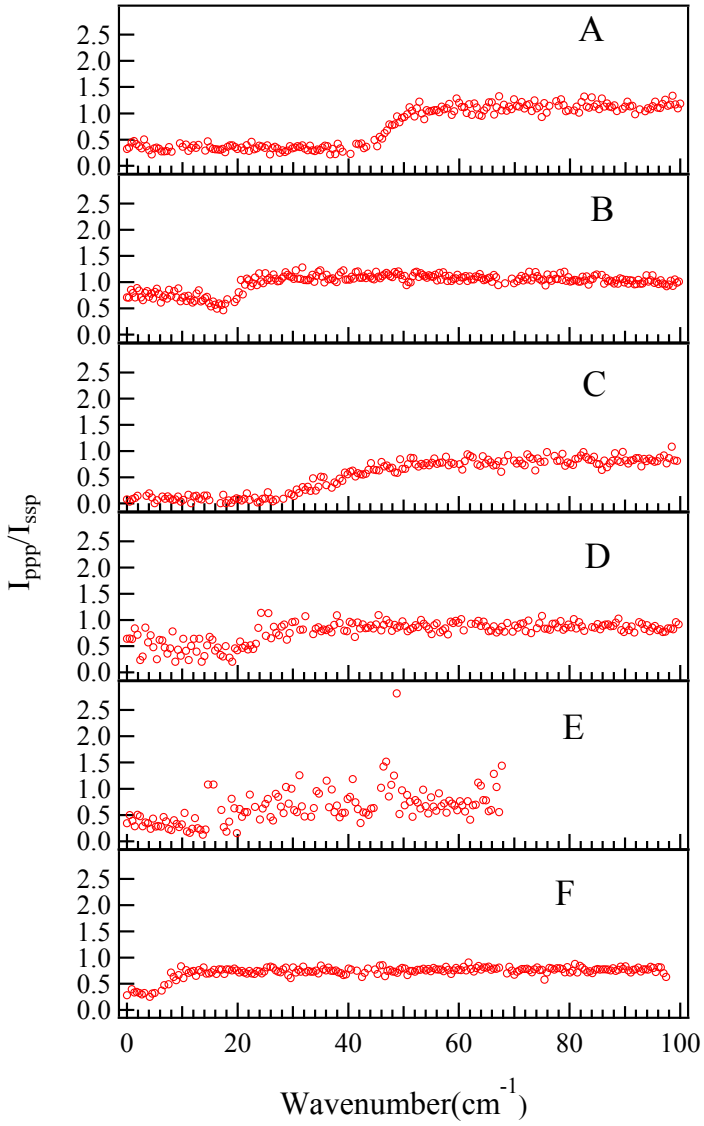

Figure S4. Time dependence of SFG signal ratio(I_{ppp}/I_{ssp}) during the adsorption of poly-dT_{25} molecules on to DMTAP bilayer at different buffer concentration. A: C_{Tris} = 0.1 mM; B: C_{Tris} = 5 mM; C: C_{Tris} = 10 mM; D: C_{Tris} = 25 mM. E: C_{Tris} = 75 mM; F: C_{MgCl_2} = 10 mM.

3. Fitting of SFG-VS Signals

As described in detail elsewhere, the intensity of the SFG light is proportional to the square of the sample's second-order nonlinear susceptibility($\chi_{eff}^{(2)}$), and the intensity of the two input

fields $I_1(\omega_{vis})$ and $I_2(\omega_{IR})$, see eq. (S1). $\chi_{eff}^{(2)}$ vanishes when the structure of contributing molecules/medium has an inversion symmetry.[5-11]

$$I(\omega_{SFG}) \propto \left|\chi_{eff}^{(2)}\right|^2 I_1(\omega_{vis}) I_2(\omega_{IR}) \qquad (S1)$$

where $\omega_{SFG} = \omega_{IR} + \omega_{vis}$. As the IR beam frequency is tuned over a vibrational resonance of surface/interface molecules, the effective surface nonlinear susceptibility can be greatly enhanced. By assuming the frequency dependence of $\chi_{eff}^{(2)}$ at the charged surface in ionic solution can be described is described by eq. (S2)

$$\chi_{eff}^{(2)}(\omega_{IR}) = \chi_{NR}^{(2)} + \chi_s^{(2)} + \chi_{EDL}^{(2)} = \chi_{NR}^{(2)} + N_s\chi_s^{(2)} + C_B\chi_B^{(3)}\frac{k}{k + i\Delta k_z}\Psi_0 \qquad (S2)$$

where $\chi_{NR}^{(2)}$ $\chi_s^{(2)}$ and $\chi_{EDL}^{(2)}$ are he non-resonant response, the response of molecules on surface, and the response of molecules in electric double layer respectively. If we assume the molecules on surface and the molecules in electric double layer has same vibrational resonance.

$$\chi_{eff}^{(2)}(\omega_{IR}) = \chi_{NR}^{(2)} + \sum_{\upsilon}\frac{A_s^{(2)} + \Psi_0 A_B^{(3)}\dfrac{k}{k + i\Delta k_z}}{\omega_{IR} - \omega_\upsilon + i\Gamma_\upsilon}$$

$$= \chi_{NR}^{(2)} + \sum_{\upsilon}\frac{A_s^{(2)}(\omega_{IR} - \omega_\upsilon) + \Psi_0[A_B^{(3)}(\omega_{IR} - \omega_\upsilon)F_1 - A_B^{(3)}\Gamma_\upsilon F_2]}{(\omega_{IR} - \omega_\upsilon)^2 + \Gamma_\upsilon{}^2} + \frac{A_s^{(2)}\Gamma_\upsilon + \Psi_0[A_B^{(3)}(\omega_{IR} - \omega_\upsilon)F_2 + A_B^{(3)}\Gamma_\upsilon F_1]}{(\omega_{IR} - \omega_\upsilon)^2 + \Gamma_\upsilon{}^2} \qquad (S3)$$

$$F_1 = \frac{k^2}{k + \Delta k_z{}^2} \qquad (S4)$$

$$F_2 = \frac{k\Delta k_z}{k + \Delta k_z{}^2} \qquad (S5)$$

where ω_υ, and Γ_υ are the resonant frequency, and damping coefficient of the vibrational mode(ν), respectively. $A_s^{(2)}$, $A_B^{(3)}$ are the amplitudes of second order susceptibility of the surface and third

order susceptibility of the EDL. $1/k$, $1/\Delta k_z$, Ψ_0 are the Debye screening length of the surface potential in the electronic diffuse layer (EDL), coherent length of the SFG process and the surface potential at the charged surface respectively.

$$\Psi_0 = \frac{2k_BT}{e}\sinh^{-1}\left(\frac{\sigma_{sum}}{\sqrt{8000k_BTN_AC\varepsilon_0\varepsilon_r}}\right) \qquad (S6)$$

$$1/k = \left(8\pi L_B c_{salt}\right)^{-\frac{1}{2}} \simeq \frac{0.304}{\sqrt{c_{salt}}}nm \qquad (S7)$$

where σ_{sum} is the summation of surface charge density, k_B, N_A are the Boltzmann constant and the Avogadro constant, ε_r and ε_0 relative dielectric constant, dielectric constant in vacuum, C is the molar electrolyte constant. The fitting parameters($1/k$, $1/\Delta k_z$, Ψ_0) in different salt concentration are listed in Table S1.The plot of SFG signal vs. the IR input frequency shows a polarization-dependent vibrational spectrum of the molecules at surface or interface. A_υ, ω_υ, and Γ_υ can be extracted by fitting the spectrum using eq.S2.

Table S1. The fitting parameters in different salt concentration.

Concentration Mol/L	$1/k$ nm	$1/\Delta k_z$ nm	Ψ_0 mV	F_1	F_2
0.0001	30.4	43	0.309	0.6769	0.4677
0.005	4.30	43	0.209	0.9905	0.0968
0.01	3.04	43	0.191	0.9952	0.0688
0.025	1.92	43	0.167	0.9981	0.0436
0.075	1.11	43	0.139	0.9994	0.0252

Table S2. The fitting parameters and calculated tilt angles of thymine groups of poly-dT_{25} molecules.

Solution	Concentration (mM)	0.1	5	10	25	75
Tris buffer	ω_υ	1659.8	1665.1	1661.1	1661.1	1662.6
	Γ_υ	24.7	20.5	18.0	18.0	15.0

	$\chi^{(2)}_{ppp}/\chi^{(2)}_{ssp}$	0.97	1.31	1.72	1.18	1.32
	Tilt Angle (º)	42.9	36.7	29.8	38.9	36.5
$MgCl_2$	ω_υ	1662.0	1669.3	1664.1	1661.7	1666.6
	Γ_υ	21.3	20.5	20.0	20.1	24.7
	$\chi^{(2)}_{ppp}/\chi^{(2)}_{ssp}$	0.81	1.06	1.07	1.72	0.68
	Tilt Angle (º)	46.3	41.2	41	29.9	49.3

4. Function for diffusion kinetics.

For the adsorption kinetic of oligonucleotides molecule from bulk solution to surface,

$$\frac{\partial c}{\partial t} = D\frac{\partial^2 c}{\partial x^2} \quad \text{(S8)}$$

$$c_0(x,t) = c_\infty erfc\left[\frac{x}{2\sqrt{Dt}}\right], \left(erfc[z] = 1 - erf[z] = \frac{2}{\sqrt{\pi}}\int_z^\infty \exp\left[-y^2\right]dy\right) \quad \text{(S9)}$$

For charged surface (where $\left.\frac{\partial c_0(x,t)}{\partial x}\right|_{z<0} = 0$), the increasing of adsorbed oligonucleotide can be described as combination of diffusion from two sources, $c_B = c_\infty, x_1 = x,\ x_2 = -x$.

$$c_S(t) = c_0(x,t) + c_0(-x,t) = 2c_B erfc\left[\frac{x}{2\sqrt{Dt}}\right] \quad \text{(S10)}$$

For OH signals in the wavenumber range of 2800-3800,

$$\chi^{(2)}_{eff} \propto \chi^{(2)}_{NR} + \sum_n \left(2\chi^{(2)}_{S,n} erfc\left[\frac{x}{2\sqrt{D_n(t-t_{n0})}}\right] + 2\chi^{(3)}_{B,n}\Psi_0\left(1 - \frac{\sigma_{dT_{25}}}{\sigma_0} erfc\left[\frac{x}{2\sqrt{D_n(t-t_{n0})}}\right]\right)\right) \quad \text{(S11)}$$

For dT signals in the wavenumber range of 2800-3800, $\chi_S^{(2)} \gg \chi_B^{(3)}$,

$$\chi_{eff} \propto \chi_{NR} + \sum_n 2\chi_{S,n}^{(2)} erfc\left[\frac{x}{2\sqrt{D_n(t-t_{n0})}}\right] \quad \text{(S12)}$$

4. Susceptibilities of molecular groups

The molecular orientation information can be obtained by relating SFG susceptibility tensor elements $\chi_{ijk}(i,j,k=x,y,z)$ in the laboratory frame to the SFG molecular hyperpolarizability tensor elements $\beta_{lmn}(l,m,n=a,b,c)$ in the molecular frame via the Euler transformation.[3,4] The Euler transformation used here follows the z-x-y convention, which has a matrix in the form shown in eq.S4.

$$\chi_{ijk,q}^{(2)} = \sum_{l,m,n} N_s \left\langle R_{il} R_{jm} R_{kn} \right\rangle \beta_{lmn,q} \quad \textit{(S13)}$$

$$R_{il,\,jm,kn} = \begin{pmatrix} -\sin(\varphi)\cos(\theta)\sin(\psi)+\cos(\varphi)\cos(\psi) & -\sin(\varphi)\cos(\theta)\cos(\psi)-\cos(\varphi)\sin(\psi) & \sin(\varphi)\sin(\theta) \\ \cos(\varphi)\cos(\theta)\sin(\psi)+\sin(\varphi)\cos(\psi) & \cos(\varphi)\cos(\theta)\cos(\psi)-\sin(\varphi)\sin(\psi) & -\cos(\varphi)\sin(\theta) \\ \sin(\theta)\sin(\psi) & \sin(\theta)\cos(\psi) & \cos(\theta) \end{pmatrix} \quad \textit{(S14)}$$

The components of $\chi_{eff}^{(2)}$ of ssp, and ppp polarization combinations are given in equations (S5)-(S6) in the lab coordinate system which is defined as the z-axis being along the surface normal and the x-axis being in the incident plane.[5-9]

$$\chi_{eff,ssp}^{(2)} = L_{yy}(\omega_{SF}) L_{yy}(\omega_{Vis}) L_{zz}(\omega_{IR}) \sin\beta_{IR} \chi_{yyz}^{(2)} \quad \textit{(S15)}$$

$$\begin{aligned} \chi_{eff,ppp}^{(2)} = & -L_{xx}(\omega_{SF}) L_{xx}(\omega_{Vis}) L_{zz}(\omega_{IR}) \cos\beta_{SF} \cos\beta_{Vis} \sin\beta_{IR} \chi_{xxz}^{(2)} \\ & - L_{xx}(\omega_{SF}) L_{zz}(\omega_{Vis}) L_{xx}(\omega_{IR}) \cos\beta_{SF} \sin\beta_{Vis} \cos\beta_{IR} \chi_{xzx}^{(2)} \\ & + L_{zz}(\omega_{SF}) L_{xx}(\omega_{Vis}) L_{xx}(\omega_{IR}) \sin\beta_{SF} \cos\beta_{Vis} \cos\beta_{IR} \chi_{zxx}^{(2)} \\ & + L_{zz}(\omega_{SF}) L_{zz}(\omega_{Vis}) L_{zz}(\omega_{IR}) \sin\beta_{SF} \sin\beta_{Vis} \sin\beta_{IR} \chi_{zzz}^{(2)} \end{aligned} \quad \textit{(S16)}$$

where β_{SF}, β_{Vis} and β_{IR} are the angles between the surface normal and the sum frequency beam, the input visible beam, and the input IR beam, respectively. L_{ii} (i = x, y or z) denotes the Fresnel coefficients.

2.1 Thymine C_4=O & C_5=C_6 in phase stretching

After considering the Fresnel coefficient constants under this experimental geometry, eqs.(S5-S6) are then given by

$$\chi^{(2)}_{\mathrm{eff,ssp}} = 1.319\chi^{(2)}_{\mathrm{yyz}} \qquad (S17)$$

$$\chi^{(2)}_{\mathrm{eff,ppp}} = -0.137\chi^{(2)}_{\mathrm{xxz}} - 0.110\chi^{(2)}_{\mathrm{xzx}} + 0.105\chi^{(2)}_{\mathrm{zxx}} + 1.184\chi^{(2)}_{\mathrm{zzz}} \qquad (S18)$$

Because $\chi^{(2)}_{xxz}$ equals to $\chi^{(2)}_{yyz}$ for C_∞ symmetry, the $\chi^{(2)}_{xxz}$ and $\chi^{(2)}_{zzz}$ susceptibility components are the main contributors to the ssp and ppp signals, respectively. With an azimuthal symmetry of the molecules at the interface, the dependence of $\chi^{(2)}_{xxz}$ and $\chi^{(2)}_{zzz}$ susceptibility components on the molecular hyperpolarizability can be described by the following equations. [5-10]

A_1 mode:

$$\begin{aligned}\chi^{(2),A1}_{xxz} = \chi^{(2),A1}_{yyz} &= \frac{1}{2}N_s\beta_{ccc}[\langle\cos^2\psi\rangle R_a + \langle\sin^2\psi\rangle R_b + 1]\langle\cos\theta\rangle \\ &+ \frac{1}{2}N_s\beta_{ccc}[\langle\sin^2\psi\rangle R_a + \langle\cos^2\psi\rangle R_b - 1]\langle\cos^3\theta\rangle\end{aligned} \qquad (S19)$$

$$\begin{aligned}\chi^{(2),A1}_{zzz} &= N_s\beta_{ccc}[\langle\sin^2\psi\rangle R_a + \langle\cos^2\psi\rangle R_b]\langle\cos\theta\rangle \\ &- N_s\beta_{ccc}[\langle\sin^2\psi\rangle R_a + \langle\cos^2\psi\rangle R_b - 1]\langle\cos^3\theta\rangle\end{aligned} \qquad (S20)$$

where ψ is the twisting angle of thymine group.

$$R_a = \frac{\beta_{aac}}{\beta_{ccc}} = \frac{\alpha^{(2)}_{aa}}{\alpha^{(2)}_{cc}} \qquad (S21)$$

$$R_b = \frac{\beta_{bbc}}{\beta_{ccc}} = \frac{\alpha^{(2)}_{bb}}{\alpha^{(2)}_{cc}} \qquad (S22)$$

According to eqs.(S18) and (S19), the deduced susceptibility ratio $\chi^{(2)}_{ppp,thymine} / \chi^{(2)}_{ssp,thymine}$ at $\psi = 0°$ can be plotted as a function of the tilt angle (shown in Figure S3).

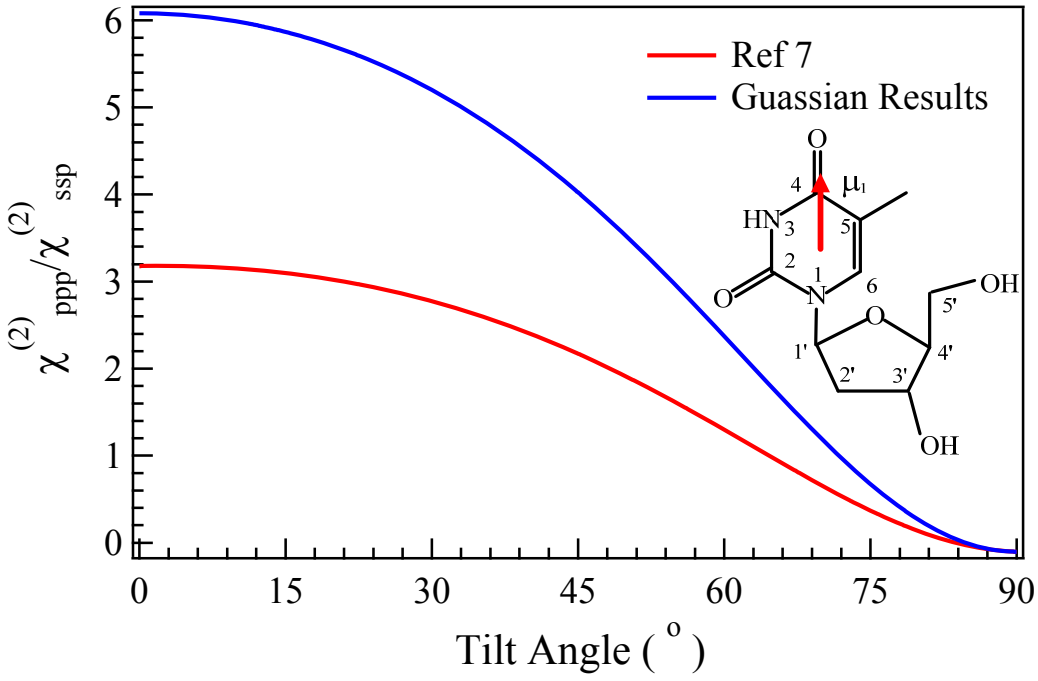

Figure S5 Simulated tile angle dependence of susceptibility ratio $\chi^{(2)}_{ppp} / \chi^{(2)}_{ssp}$ C4=O & C5=C6 in phase stretching of thymine group.

The Raman tensors of thymidine groups at 1665 cm^{-1} has been reported in previous literatures(C1 coordinates, $\frac{\alpha^{(2)}_{aa}}{\alpha^{(2)}_{cc}}$ = 4.31, $\frac{\alpha^{(2)}_{bb}}{\alpha^{(2)}_{cc}}$ = 0.25).[7] The molecular coordinate is determined by taking the plane of thymine aromatic ring as bc plane and taking the $\vec{\mu}_{C_4=O}$ vector as c-axis. The IR dipole moment at wavenumber of C_4=O & C_5=C_6 in phase mode either can be the same as the vector of C_4=O bond or can be calculated using the vibration displacements of each atom ($\frac{\partial x}{\partial Q}, \frac{\partial y}{\partial Q}, \frac{\partial z}{\partial Q}$) listed in the Guassian output file (*.out or *.gjy). [14]

$$\frac{\partial \vec{\mu_Q}}{\partial Q} = \sum_n M_n \left(\frac{\partial x}{\partial Q}\frac{\partial \mu_n}{\partial x}\vec{x} + \frac{\partial y}{\partial Q}\frac{\partial \mu_n}{\partial y}\vec{y} + \frac{\partial z}{\partial Q}\frac{\partial \mu_n}{\partial z}\vec{z} \right) \qquad (S23)$$

Where M_n is the relative mass of each atom, $\frac{\partial \mu_n}{\partial x}$, $\frac{\partial \mu_n}{\partial y}$ and $\frac{\partial \mu_n}{\partial z}$ are the dipole derivatives of each atom listed at the end of Guassian output file.

Table S3. Derivatives of Raman tensors and IR transition dipoles of C_4=O & C_5=C_6 in phase stretching mode at 1665 cm^{-1}.

Vibrational mode	$\frac{\partial \alpha_{\text{Raman}}}{\partial Q}$	$\frac{\partial \mu_{\text{IR}}}{\partial Q}$	Transformation Matrix
Data from Ref. 7	$\begin{vmatrix} \frac{1}{4.31} & 0 & 0 \\ 0 & \frac{0.25}{4.31} & 0 \\ 0 & 0 & 1 \end{vmatrix}$	$\begin{vmatrix} 0 \\ 0 \\ 1 \end{vmatrix}$	$\begin{vmatrix} 0 & 0 & 1 \\ 0 & 1 & 0 \\ 1 & 0 & 0 \end{vmatrix}$
Calculated Results*	$\begin{vmatrix} 0.329 & 0.137 & -0.283 \\ 0.137 & 0.127 & -0.142 \\ -0.283 & -0.142 & 0.834 \end{vmatrix}$	$\begin{vmatrix} 0 \\ 0 \\ 1 \end{vmatrix}$	$\begin{vmatrix} 0.067 & 0.014 & 0.998 \\ -0.220 & -0.975 & 0.029 \\ 0.973 & -0.222 & -0.062 \end{vmatrix}$

*The derivatives of IR dipole of Thymidine groups was calculated by Guassian 09 using Hartree-fork method with 3-21G+** basis.[14]

Reference

1. Gonella, G.; Lütgebaucks, C.; de Beer, A. G. F.; Roke, S., Second Harmonic and Sum-Frequency Generation from Aqueous Interfaces Is Modulated by Interference. *J. Phys. Chem. C* **2016**, *120*, 9165-9173.
2. Wang, H. F., Sum frequency generation vibrational spectroscopy (SFG-VS) for complex molecular surfaces and interfaces: Spectral lineshape measurement and analysis plus some controversial issues. *Prog. Surf. Sci.* **2016**, *91*, 155-182.
3. Eftekhari-Bafrooei, A.; Borguet, E., Effect of Electric Fields on the Ultrafast Vibrational Relaxation of Water at a Charged Solid–Liquid Interface as Probed by Vibrational Sum Frequency Generation. *J. Phys. Chem. Lett.* 2011, *2*, 1353-1358.

4. Nihonyanagi, S.; Yamaguchi, S.; Tahara, T., Water Hydrogen Bond Structure near Highly Charged Interfaces Is Not Like Ice. *J. Am. Chem. Soc.* **2010,** *132*, 6867-6869.

5. Y. R. Shen, The Principles of Nonlinear Optics, 1st ed; John Wiley& Sons: New York, 1984.

6. Moad, A. J.; Simpson, G. J. A Unified Treatment of Selection Rules and Symmetry Relations for Sum-Frequency and Second Harmonic Spectroscopies. *J. Phys. Chem. B* **2004**, *108*, 3548-3562.

7. Chen, X.; Wang, J.; Boughton, A. P.; Kristalyn, C. B.; Chen, Z. Multiple Orientation of Melittin inside a Single Lipid Bilayer Determined by Combined Vibrational Spectroscopic Studies. *J. Am. Chem. Soc.* **2007**, *129*, 1420-1427.

8. Wang, J.; Lee, S. H.; Chen Z. Quantifying the Ordering of Adsorbed Proteins in Situ. *J. Phys. Chem. B* **2008**, *112*, 2281-2290.

9. Nguyen, K. T.; Le Clair, S. V.; Ye, S.; Chen, Z. Orientation Determination of Protein Helical Secondary Structures Using Linear and Nonlinear Vibrational Spectroscopy. *J. Phys. Chem. B* **2009**, *113*, 12169-12180.

10. Lee, S.; Wang, J.; Krimm, S.; Chen, Z. Quantifying the Ordering of Adsorbed Proteins In Situ. *J. Phys. Chem. A* **2006**, *110*, 7035-7044.

11. Thomas, G. J., Jr.; Benevides, J. M.; Overman, S. A.; Ueda, T.; Ushizawa, K.; Saitoh, M.; Tsuboi, M., Polarized Raman spectra of oriented fibers of A DNA and B DNA: anisotropic and isotropic local Raman tensors of base and backbone vibrations. *Biophys. J.* **1995,** *68*, 1073-1088.

12. Benevides, J. M.; Overman, S. A.; Thomas, G. J., Raman, polarized Raman and ultraviolet resonance Raman spectroscopy of nucleic acids and their complexes. *J. Raman Spectrosc.* **2005,** *36*, 279-299.

13. Casillas-Ituarte, N. N.; Chen, X.; Castada, H.; Allen, H. C., Na(+) and Ca(2+) effect on the hydration and orientation of the phosphate group of DPPC at air-water and air-hydrated silica interfaces. *J. Phys. Chem. B* **2010,** *114*, 9485-9495.

14. Gaussian 09, Revision D.01, Frisch, M. J.; Trucks, G. W.; Schlegel, H. B.; Scuseria, G. E.; Robb, M. A.; Cheeseman, J. R.; Scalmani, G.; Barone, V.; Mennucci, B.; Petersson, G. A.; Nakatsuji, H.; Caricato, M.; Li, X.; Hratchian, H. P.; Izmaylov, A. F.; Bloino, J.; Zheng, G.; Sonnenberg, J. L.; Hada, M.; Ehara, M.; Toyota, K.; Fukuda, R.; Hasegawa, J.; Ishida, M.; Nakajima, T.; Honda, Y.; Kitao, O.; Nakai, H.; Vreven, T.; Montgomery, J. A., Jr.; Peralta, J. E.; Ogliaro, F.; Bearpark, M.; Heyd, J. J.; Brothers, E.; Kudin, K. N.; Staroverov, V. N.; Kobayashi, R.; Normand, J.; Raghavachari, K.; Rendell, A.; Burant, J. C.; Iyengar, S. S.;

Tomasi, J.; Cossi, M.; Rega, N.; Millam, M. J.; Klene, M.; Knox, J. E.; Cross, J. B.; Bakken, V.; Adamo, C.; Jaramillo, J.; Gomperts, R.; Stratmann, R. E.; Yazyev, O.; Austin, A. J.; Cammi, R.; Pomelli, C.; Ochterski, J. W.; Martin, R. L.; Morokuma, K.; Zakrzewski, V. G.; Voth, G. A.; Salvador, P.; Dannenberg, J. J.; Dapprich, S.; Daniels, A. D.; Farkas, Ö.; Foresman, J. B.; Ortiz, J. V.; Cioslowski, J.; Fox, D. J. Gaussian, Inc., Wallingford CT, **2009**.